Chemical Physics Letters 691 (2018) 341–346

Contents lists available at ScienceDirect

Chemical Physics Letters

journal homepage: www.elsevier.com/locate/cplett

Research paper

Structural, electronic and photocatalytic properties of atomic defective BiI_3 monolayers

Huang Yan, Hu Ziyu *, Gong Xu, Shao Xiaohong *

College of Science, Beijing University of Chemical Technology, Beijing 100029, China

ARTICLE INFO

Article history:
Received 23 October 2017
In final form 20 November 2017
Available online 22 November 2017

Keywords:
Defective structures
BiI_3 monolayer
Electronic properties
Photocatalytic properties

ABSTRACT

The structural, electronic and photocatalytic properties of five vacancy-containing 2D BiI_3 monolayers are investigated by the first-principle calculations. The electronic structures show that the five structures are stable and have comparable binding energies to that of the pristine BiI_3 monolayer, and the defects can tune the band gaps. Optical spectra indicate that the five structures retain high absorption capacity for visible light. The spin-orbit coupling (SOC) effect is found to play an important role in the band edge of defective structures, and the V_{Bi} and $V_{Bi\text{-}I3}$ defective BiI_3 monolayers can make absolute band edges straddle water redox potentials more easily.

1. Introduction

Solar energy is one of the most important renewable energy resources for its wide availability and environmental friendliness. The development of novel lowcost and highly efficient solar energy conversion materials is the most important task for its real applications. The 2D materials such as graphene, boron nitride and transition metal dichalcogenides have considered as good candidates for their high power conversion efficiency and better stability [1–13]. Recently, the metal halide Bismuth tri-iodide (BiI_3) compound has been investigated as gamma-ray detection primarily due to the high atomic numbers of the constituent elements and high mass density, and also has good optoelectronic properties [14–18]. BiI_3 crystallizes in an ABC stacking order layered structure, in which the I–Bi–I trilayers stacked along the [0 0 1] direction in a hexagonal lattice with a large van der Waals gap [19,20]. The structural, electronic and optical properties of bulk BiI_3 crystal have been reported both experimentally and theoretically [14,21,22]. Lehner et al. [16] have determined the absolute band positions of BiI_3 and suggested its promising optoelectronic properties. Guided by the predictive discovery framework, Brandt et al. [17] also considered BiI_3 as a candidate for thin-film photovoltaic (PV) absorbers. Very recently, Zhang et al. [23] have investigated BiI_3 and its single layer theoretically, and found that the single-layer BiI_3 possesses an electronic gap of about 1.63 eV and high absorption for visible light, which provide useful guidelines for the experimental synthesis of BiI_3 monolayer and facilitate their practical applications. However, defects are inevitable in synthesis or processing, even sometimes created intentionally, they can usually play an important role to modulate their properties such as tailoring various electronic and optical properties of two-dimensional materials and have been the subject of intense research over the last few decades [24–32]. The most common and energetically favorable types of impurities are vacancy defects (VDs) [27]. Despite the single-layer BiI_3 has been considered as a promising candidate for future low-dimensional solar energy conversion applications, vacancy defects in BiI_3 monolayer have been barely explored.

In this work, five types of VDs: (i) Bi vacancy (V_{Bi}), (ii) a vacancy complex of Bi and nearby three monoiodine vacancy ($V_{Bi\text{-}I3}$), (iii) monoiodine vacancy ($V_{I\text{-}1}$), (iv) two-monoiodine vacancy ($V_{I\text{-}12}$) and (v) three-monoiodine vacancy ($V_{I\text{-}123}$) in (SL) BiI_3 are investigated using first-principles calculations. The structural, electronic and photocatalytic properties are performed and the results show that these five defective BiI_3 monolayers can modulate the band gaps and retain good absorption for visible light. The BiI_3 monolayers with Bi vacancy (V_{Bi}) and vacancy complex ($V_{Bi\text{-}I3}$) defects are predicted to upshift the conduction band edge and could make absolute band edges straddle water redox potentials more easily relative to the pristine monolayer BiI_3.

2. Computational methods

All the calculations are performed by the projector augmented plane-wave (PAW) method [33] based on density functional theory (DFT) in the Vienna Ab initio Simulation Package (VASP) [34,35].

* Corresponding authors.
E-mail addresses: huziyu@mail.buct.edu.cn (H. Ziyu), shaoxh@mail.buct.edu.cn (S. Xiaohong).

https://doi.org/10.1016/j.cplett.2017.11.044
0009-2614/

The exchange and correlation potential are described by generalized gradient approximation in the Perdew Burkee Ernzerhof (GGA-PBE) form [36]. To simulate the long-range van der Waals interaction, a dispersion correction of the total energy of Grimme's pair-wise correction (DFT-D3) [37], the Tkatchenko and Scheffler van der Waals correction (vdW-TS) [38] methods and optimized Becke88 van der Waals (optB88-vdW) [39,40] functional are also employed for comparison. To evaluate the importance of the spin-orbit coupling (SOC) effect, we perform comparative calculations for BiI_3 with and without SOC. The projector augmented wave (PAW) pseudopotential is treated as $6s^26p^3$ and $5s^25p^5$ for Bi and I, respectively. A plane-wave basis set with a cutoff energy of 500 eV is used in the calculation. All the structures are fully relaxed with a force tolerance of 0.01 eV/Å. K-Points with a mesh of $13 \times 13 \times 1$ and $7 \times 7 \times 1$ generated by the scheme of Monkhorst–Pack [41] are used for pristine and defective BiI_3 monolayer geometry optimization and optical property calculations, respectively. To study 2D systems under the periodic boundary conditions, a vacuum layer with a thickness of at least 20 Å is inserted to avoid the interaction between periodic images, and a hexagonal supercell $6 \times 6 \times 1$ is adopted and five types of vacancy defects are introduced.

3. Results and discussion

3.1. Structure of pristine and different types of vacancy defects (SL) BiI_3

We firstly calculated the bulk BiI_3 (Fig. 1) and a $6 \times 6 \times 1$ supercell of pristine BiI_3 monolayer (see Fig. 2a). The corresponding lattice constants of the fully relaxed structures are list in Table 1. As is seen, compared with the experimental results, the PBE functional significantly overestimates the lattice parameters a or b and c by about 4%, 11%, respectively, which are all consistent with the previous calculations for bulk BiI_3 [23]. Due to BiI_3 consists of I–Bi–I trilayers binding with weak vdW interaction, and we thus use optB88-vdW to investigate the structure of BiI_3, the calculated lattice constants of the bulk BiI_3 and pristine single-layer BiI_3 are 7.531 Å and 7.548 Å, respectively, which are good agreement with previously calculated value [23]. In addition, the volumes and lattice parameters predicted by vdW-D3 or vdW-TS approach in PBE are closer to the experimental values [42,43]. Therefore, we can conclude that the vdW-D3 and vdW-TS approximations are suitable for BiI_3. However, the calculated lattice constants of bulk BiI_3 and pristine single-layer BiI_3 with vdW-TS correlation is 7.628 Å and 7.635 Å, respectively, which also overestimates the lattice parameters slightly than that of the optB88-vdW method. Finally, the calculated lattice constants of the bulk BiI_3 and pristine single-layer BiI_3 by DFT-D3 approach decrease from 7.838 Å to 7.518 Å and 7.812 to 7.545 Å, respectively, which are much closer to the experimental value for bulk BiI_3.

Subsequently, we evaluate the possible vacancies defects in BiI_3 monolayers, and the optimized structures of V_{Bi}, $V_{Bi\text{-}I3}$, $V_{I\text{-}1}$, $V_{I\text{-}12}$ and $V_{I\text{-}123}$ are shown in Fig. 2b–f, respectively. Fig. 2b and d are the V_{Bi} and $V_{I\text{-}1}$ defective structures, which are constructed by removing one Bi atom or I atom from the pristine BiI_3 monolayers, as a results, which have slight effect on the structure. Fig. 2c, e and f are the other three defective BiI_3 monolayers, named $V_{Bi\text{-}I3}$, $V_{I\text{-}12}$ and $V_{I\text{-}123}$, resulting from the lack of one Bi atom with nearby three I atoms, two and three I atoms, respectively. As is seen, most of the atoms have a significant displacement, especially around the vacancies, resulting in local distorted hexagons. Furthermore, in the $V_{I\text{-}1}$, $V_{I\text{-}12}$ and $V_{I\text{-}123}$ defective systems, the Bi–I bond length around vacancy gets longer gradually. To check the stability of these defects in BiI_3 monolayers, the calculated binding energies (E_b) for all the typical vacancy defects are summarized in Table 2. E_b is defined as $E_b = [nE_{(Bi)} + mE_{(I)} - E_{(BiI3)}]/(n + m)$, where $E_{(Bi)}$ and $E_{(I)}$ are the average energy per bismuth and iodine atom, respectively. n and m denote the number of bismuth atoms and iodine atoms in the pristine or defective (SL) BiI_3, and $E_{(BiI3)}$ is the total energy of the supercell with or without defects. Since the strong SOC effect is expected in BiI_3 [23,43], we also calculate the binding energies of pristine and defective (SL) BiI_3 using the PBE and PBE + SOC. The energies calculated by PBE, PBE + SOC, DFT-D3 and vdW-TS methods are positive vary from 0.698 to 1.135 eV, which indicates that pristine and defective (SL) BiI_3 are stable. In addition, the V_{Bi} defect is the most stable in these five defective structures. In the $V_{I\text{-}1}$, $V_{I\text{-}12}$ and $V_{I\text{-}123}$ defective systems, with the increase of I vacancies, the binding energies decrease gradually, implies that the $V_{I\text{-}123}$ defective structure is more stable than the other two monoiodine vacancy defect structures.

3.2. Electronic structures and optical properties

The calculated bandgaps of the five defective structures calculated by various methods are listed in Table 3. For comparison, we first check the band gap of pristine BiI_3 monolayer. The obtained indirect band gap of pristine BiI_3 monolayer are 2.58, 1.58, 2.54 and 2.53 eV from PBE, PBE + SOC, DFT-D3 and vdW-TS methods, respectively. The calculated bandgap of 1.58 eV by PBE + SOC is rather closer to the experimental value of 1.67 eV [15] and the previous calculated value of 1.63 eV [23]. Due to the existence of strong spin orbit effect in BiI_3 monolayer, and the SOC effect should be considered for the bandgap calculation. The results

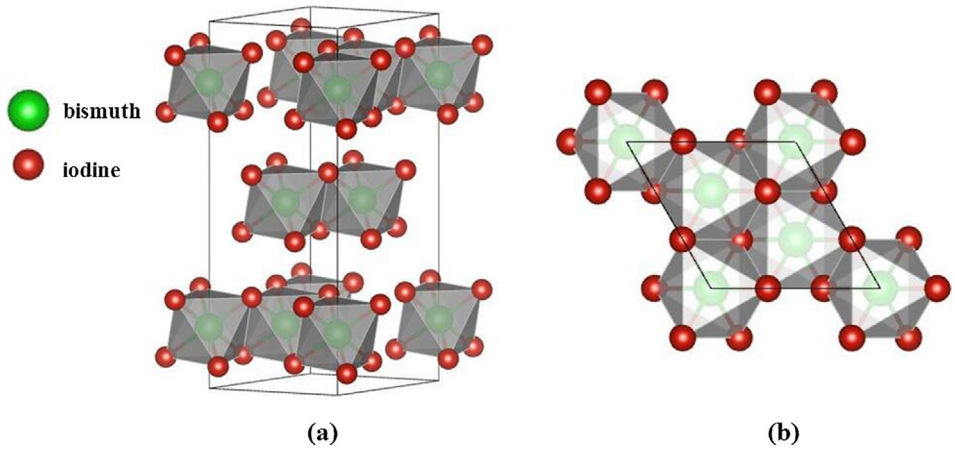

Fig. 1. The crystal structure in hexagonal (a) side view and (b) top view of bulk BiI_3.